The Biomechanics of Erections: Two- Versus One-Compartment Pressurized Vessel Modeling of the Penis

Ahmed M. Mohamed
Department of Mechanical Engineering,
University of Minnesota,
1400 S. 2nd Street, Apartment A907,
Minneapolis, MN 55454
e-mail: moha0128@umn.edu

Arthur G. Erdman
Department of Mechanical Engineering,
University of Minnesota,
111 Church Street SE,
Minneapolis, MN 55455
e-mail: agerdman@umn.edu

Gerald W. Timm
Department of Urologic Surgery,
Academic Health Center,
University of Minnesota,
D510 Mayo Memorial Building,
420 Delaware Street SE,
Minneapolis, MN 5455
e-mail: timmx025@tc.umn.edu

Previous biomechanical models of the penis simulated penile erections utilizing 2D geometry, simplified 3D geometry or made inaccurate assumptions altogether. These models designed the shaft of the penis as a one-compartment pressurized vessel fixed at one end when in reality it is a two-compartment pressurized vessel in which the compartments diverge as they enter the body and are fixed at two separate anatomic sites. This study utilizes the more anatomically correct two-compartment penile model to investigate erectile function. Simplified 2D and 3D models of the erect penis were developed using the finite element method with varying anatomical considerations for analyzing structural stresses, axial buckling, and lateral deformation. This study then validated the results by building and testing corresponding physical models. Finally, a more complex and anatomically accurate model of the penis was designed and analyzed. When subject to a lateral force of 0.5 N, the peak equivalent von Mises (EVM) stress in the two-compartment model increased by about 31.62%, while in the one-compartment model, the peak EVM stress increased by as high as 70.11%. The peak EVM stress was 149 kPa in the more complex and anatomically accurate penile model. When the perforated septum was removed, the peak EVM stress increased to 455 kPa. This study verified that there is significant difference between modeling the penis as a two- versus a one-compartment pressurized vessel. When subjected to external forces, a significant advantage was exhibited by two corporal based cavernosal bodies separated by a perforated septum as opposed to one corporal body. This is due to better structural integrity of the tunica albuginea when subjected to external forces. [DOI: 10.1115/1.4002794]

1 Introduction

Penile erection usually follows sexual stimulation of the visual, auditory, and/or tactile senses. Therefore, normal erections depend on an intact central nervous system and on the intactness of various autonomic nerves and arteries/veins to supply and drain blood in and out of the penis [1,2]. Erectile dysfunction, also known as impotency, is the inability to develop and maintain an erection adequate for vaginal intromission. Studies have indicated that the prevalence of erectile dysfunction significantly increases with age and that it is more of a physical phenomenon than a psychological one [3–5]. A community-based study, which surveyed 1290 men aged 40–70 years, showed that approximately 40% of men would experience some level of erectile dysfunction at age 40, while the prevalence rate increased to almost 70% at age 70. By extrapolating these results, it is estimated that at least 30 million men suffer from some form of erectile dysfunction, with 617,715 new cases reported annually in the United States alone [3].

The human penis consists of two main functional compartments (Fig. 1(*a*)): the paired dorsally located corpora cavernosa, which consist of erectile tissue that takes up the majority of the volume within the penis, and a ventral corpus spongiosum that surrounds the urethra [1,2,6]. A thick fibrous membrane called the tunica albuginea surrounds and supports each of the corporal bodies [1,2]. The corpora cavernosa lie in intimate apposition along the shaft of the penis and share a perforated septum. The corporal bodies, however, begin to separate at the junction of the penis within the body, as shown in Fig. 1(*b*). The corporal bodies diverge into the crura and firmly attach to the rami of the pubic arch.

Studies have shown the average outside-body length of an erection to vary from 128.9 mm to 155.0 mm with approximately one-third to one-half of the total penis length inside the body [2]. The tunica albuginea, a bilayered structure containing mostly collagen and some elastin fibers [1,7], is a 3D structure that provides great flexibility, rigidity, and tissue strength to the penis [8]. The collagen fibers have a tensile strength greater than steel, while the elastin fibers are capable of stretching to 150% of their normal length. The unique combination of these two elements produces a tunica tissue that is strong yet compliant [8]. The tunica albuginea has an average thickness of 2.4 mm [1,8] with a tensile strength of 200 kPa, a Young's modulus of 12 MPa, and a Poisson's ratio of 0.4 [9].

Describing the mechanical behavior of the erect penis enhances the understanding of normal sexual function of the penis and contributes to a better comprehension of the various conditions of erectile dysfunction. However, it is not possible to take direct measurement of internal mechanical behavior/properties of the penis in vivo with existing technology. For example, it is not possible to measure the internal stress distributions within and between the penile tissues. The computer modeling approach has the potential to fix this gap with its capability of allowing the development of biomechanical models of the human penis. Computational simulations based on these models will help us investigate and better understand the mechanisms of erectile dysfunction and explore advanced treatment approaches.

A number of studies have been done to simulate penile erections using the computer modeling approach, but most of the previous biomechanical models have either been limited to two-dimensional (2D) geometry, simplified three-dimensional (3D)

Contributed by the Bioengineering Division of ASME for publication in the JOURNAL OF BIOMECHANICAL ENGINEERING. Manuscript received June 22, 2009; final manuscript received October 11, 2010; accepted manuscript posted October 15, 2010; published online November 8, 2010. Assoc. Editor: Jacques M. Huyghe.

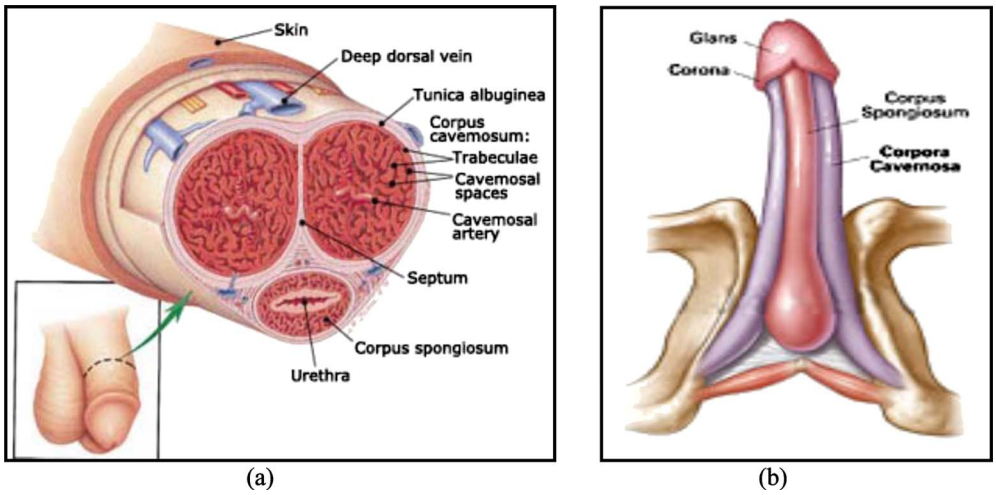

Fig. 1 (*a*) **Cross section of the human penis locating the corpus cavernosa, corpus spongiosum, urethra, and tunica albuginea (from and with permission of www.penishints.com). (*b*) Anatomy of the human penis illustrating the divergence of the corporal bodies as they enter the body and attach at the pubic ramus (from and with permission of www.vig-rxreview.com).**

geometry, or made inaccurate assumptions altogether [4,6,10,11]. Gefen et al. developed a 2D biomechanical model for the analysis of mechanical stresses in the penile tissues [10]. Fibrous plaques, a result of Peyronie's disease, were included in the model and the corresponding analysis of the stress distributions was also conducted for this disease. However, as a 2D model, it had limitations such as the inability to apply axial loads that would be present during intercourse. Linder-Ganz et al. developed a 3D biomechanical model of the penis in order to analyze tissue stresses during normal and abnormal erections [11]. The limitation of this model is that it only considered the section of the penis outside the body and did not take into account the complete and true structure of the penis, which includes the diverging crura attached at the pubic ramus. Udelson developed a biomechanical model for penile buckling based on Euler's formula for a column, in which the penis was modeled as an isotropic shaft pinned at one end [4]. However, as a biological organ that can change volume up to 300% during tumescence, it is more appropriate to model the penis as a pressurized vessel as opposed to a shaft [6]. Furthermore, the penis is better modeled as two corporal bodies that diverge inside the body and are fixed at two locations as opposed to one. Elayaperumal et al. conducted a biomechanical analysis of erectile function and compared penile buckling behavior under axial loading with radial compression [6]. They modeled the penis as a one-compartment pressurized vessel in their study; however, a two-compartment pressurized vessel in which the compartments diverge as they enter the body and are fixed at two separate points would better model the anatomical structure of the penis and would likely yield more meaningful results.

In the present study, a geometrically/anatomically correct two-compartment penile model has been developed using a computer modeling approach to study the physical, biological, and mechanical interactions within the penis, and the results were validated using physical experimental measurements. For the first time, the differences between modeling the penis as a one-compartment pressurized vessel versus a more geometrically/anatomically correct two-compartment pressurized vessel has been investigated.

2 Materials and Methods

In this study, the average outside length of 152.4 mm and the inside length of 76.2 mm were modeled for the penis using the finite element (FE) method, thus assuming that one-third of the penile length is inside the body.

2.1 Simplified Geometric FE Penile Models. Simplified geometric FE models were developed to analyze the stresses, buckling load, and lateral deformation of various penile structures and to compare the results. The corporal bodies were simplified to cylindrical shapes with varying anatomical parameters for analyzing structural stresses, axial buckling, and lateral deformation. The commercial FE analysis software package ANSYS (ANSYS Inc., Canonsburg, PA) was used to design three different models. The first model was a geometrically correct model with two cylinders representing the corporal bodies, which diverged as they entered the body and were fixed at two separate proximal ends. This model is referred to as the "two-compartment diverging" model. In the second model, the penis was designed with one pressurized cylindrical body whose cross-sectional area was equal to that of the two corporal bodies' total cross-sectional areas. This model is referred to as the "one-compartment same cross-sectional area" model. In the third model, the penis was designed with one pressurized cylindrical body whose circumference was equal to the total circumference of the two corporal bodies' total circumferences. This model is referred to as the "one-compartment same circumference" model.

The average penile implant placed inside the corpus of a patient suffering from erectile dysfunction is 12 mm in diameter [6]; therefore, penile diameters of 10 mm, 12 mm, and 14 mm were considered for the two-compartment models and their equivalent one-compartment same cross-sectional area and one-compartment same circumference models to better understand the sensitivity of the results in response to mild changes in the size of the corpora cavernosa. The thickness of the cylindrical models was 2.4 mm, which was based on the average thickness of the tunica albuginea [1,8]. The total length of the models was 228.6 mm. The two cylinders in the two-compartment diverging models diverged at a length of 152.4 mm, while the length of the curved cylinder, which represents the crura inside the body, was 76.2 mm. The distance between the attachment points of the two corporal bodies was found to be approximately 60 mm.

The tunica albuginea was assumed to be an isotropic, linear elastic material, which obeyed the following constitutive law in its tensor form in Eq. (1) [12]. The model was meshed using a four-node tetrahedron element (Solid 72) in ANSYS, and the FE meshes were systematically refined until a minimal change in results (2–5% difference in the von Mises stresses) was achieved,

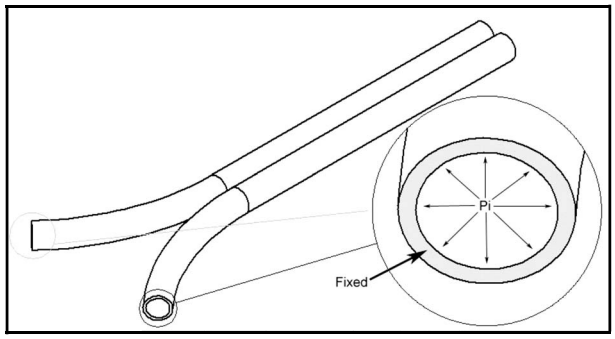

(a)

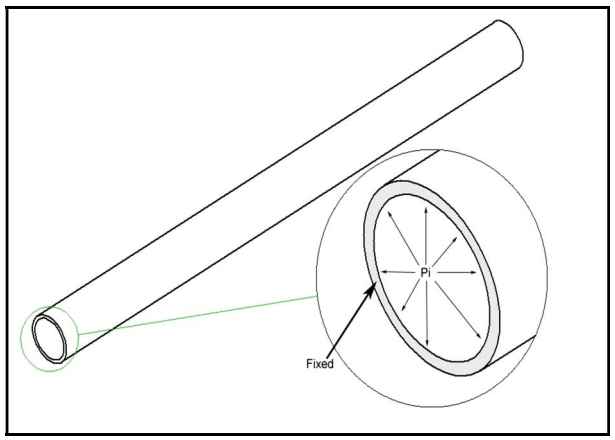

(b)

Fig. 2 Schematic drawing of boundary conditions of (*a*) two-compartment model and (*b*) same cross-sectional area and same circumference model

$$\varepsilon_{ij} = \frac{1+v}{E}\vartheta_{ij} - \frac{v}{E}\vartheta_{ij}\delta_{ij} \tag{1}$$

where E is Young's modulus and v is Poisson's ratio for the corresponding materials. The material properties discussed earlier were applied to the tunica albuginea. A Young's modulus of 12 MPa and a Poisson's ratio of 0.4 were applied [9].

Four FE analysis jobs with different boundary condition settings were conducted for each of these three models. The boundary conditions included fixed supports and an internal pressure of 13.32 kPa (100 mm Hg), as illustrated in Fig. 2 in the first FE analysis job. In the second FE analysis job, the boundary condition is an axial force of 5 N applied to the tip of the penis. The axial force was replaced by a lateral force of 0.5 N and applied on a circular cross-sectional area of 10 mm on the tip of the penis as the boundary condition in the third FE analysis job. In the fourth FE analysis job, an ANSYS program named "BUCKLING ANALYSIS" was applied as the boundary condition in which ANSYS gradually increased the applied load until a load level was achieved whereby the structure becomes unstable, and a small increase in the load caused a very large deflection. Results from the second FE analysis job were used as the initial conditions in the fourth FE analysis job. The peak equivalent von Mises (EVM) stress, lateral deformation, and buckling load were pulled out for each boundary condition from the FE analysis results. The peak EVM stress is used in many failure or yield criteria. This stress represents a uniaxial equivalent of the multi-axial stress state that the pressurized vessels experienced. Since the assumption is that the tunica albuginea will fail at 200 kPa, which is referred to as the critical stress (σ_{crit}), it will be presumed that the pressurized finite element analysis (FEA) penile models will fail when the equivalent stress (σ_e) is greater or equal to the critical stress [13].

2.2 Physical Penile Models and Validation Study. In order to validate the results obtained from the simplified geometric FE models, physical models were developed correspondingly. Three cylindrical models were fabricated out of acrylonitrile butadiene styrene (ABS) plastic (Stratasys, Inc., Eden Prairie, MN) using a rapid prototyping (RP) machine (Stratasys Dimension 1200es, Stratasys, Inc.), and each of them was coated with a thin layer of petroleum jelly. The cylinders were carefully wrapped in bandages with fiber alignment similar to that of the tunica albuginea creating a sleeve like assembly with a thickness of about 2.4 mm. The petroleum jelly facilitated the removal of the sleeve from the fabricated model. The inner layer, composed of elastic first aid tape (Nexcare Athletic Wrap, 3M, St. Paul, MN), had an expandability characteristic similar to that of the tunica albuginea [6]. The outer layer composed of a cloth bandage (Kling Gauze Roll bandage, Johnson & Johnson, New Brunswick, NJ) limited the expandability of the vessel, again, similar to the outer layer of the tunica albuginea. For the two-compartment models, the procedure was repeated twice to fabricate two identical sleeves. The two sleeves were then placed side-by-side and fixed together with another layer of cloth bandage wrap.

A nonlubricated condom (Trojan Nonlubricated, Trojan, Princeton, NJ) was then placed inside each sleeve. The sleeves were slipped onto the end of a H_2O column manometer. The sleeves were clamped with an adjustable clamp to ensure that no water leakage occurred. The column manometer was then filled with water to a height of equivalent to 100 mm Hg, which in turn filled up the sleeves with an applied internal pressure of approximately 13.32 kPa. The conjunction of the sleeve with the H_2O column was firmly fixed in all directions and in the case of the two-compartment models the distance between the attachment points of the two sleeves was 60 mm.

Once the sleeve was firmly attached to the column, a lateral deformation test was performed. As illustrated in Fig. 3(*a*), a digital force gauge (DPS-11, Imada, Inc., Northbrook, IL) was used to apply a 0.5 N lateral force at the tip of the physical model, just like in the FEA model, and the displacement of the tip was recorded. The test was repeated five times for each model. An axial load was then applied at the tip of the penis using the digital force gauge in order to measure the buckling load (Fig. 3(*b*)). The buckling load was measured by setting the force gauge's "peak mode" on. This mode continuously updated the force gauge reading with the largest force applied. Hence, an increasing axial load was applied until the force recorded by the force gauge reached a maximum. This test was also repeated five times for each model.

2.3 Advanced Anatomically Correct FE Penile Model. An advanced anatomical correct FE penile model, which represents the most anatomically correct model of the penis to the best of our knowledge, was developed, and the key differences between having two pressurized corporal bodies fixed at the pubic ramus and one pressurized corporal body fixed at one end were analyzed. A biomechanical model based on the model by Gefen et al. was modeled [10]. The dimensions of their 2D model were measured then redesigned in ANSYS. The 2D design was then extruded into a 3D model, with the two corporal bodies diverging as they entered the body. Again, each corporal body was fixed at one end, an internal pressure of 13.32 KPa was applied inside the corporal bodies, and the peak EVM stress was analyzed. The skin was introduced in this model with a Young's modulus and a Poisson's ratio of 0.5 MPa and 0.4, respectively [14]. Finally, the septum between the two corporal bodies in the 2D model was removed. The 2D model was then extruded into a 3D model, fixed at one end, the peak EVM stress was analyzed and a BUCKLING ANALYSIS was conducted, and the results of both models were then compared side-by-side.

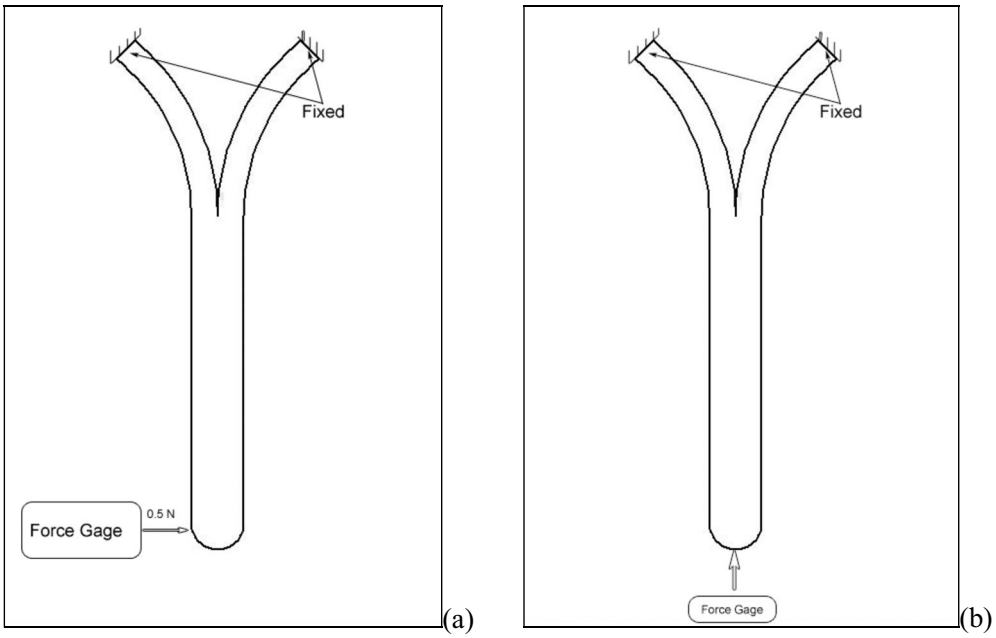

Fig. 3 Schematic drawing of (*a*) applying a lateral force in the direction of the arrow to the tip of the penis model and (*b*) applying an axial force in the direction represented by the arrow to test the buckling load of the physical model

3 Results

3.1 Simplified Geometric FE Penile Models. Figure 4(*a*) shows the FE mesh of the 12 mm two-compartment diverging model using a tetrahedron solid element for a total of 50,360 elements and 95,651 nodes (exported from ANSYS, side-by-side with its respective mesh). The EVM stress distributions throughout this 12 mm 3D two-compartment diverging model, induced by applying an internal pressure of 13.32 kPa, are shown in Fig. 4(*b*). The two-compartment diverging model experienced maximum and minimum stresses of 67,735 Pa and 54.546 Pa, respectively. Distributions of the EVM stresses over 50 kPa induced by applying an internal pressure of 13.32 kPa in the above 12 mm 3D two-compartment diverging simplified tunica albuginea model are shown in Fig. 5(*a*). For comparison, distributions of the EVM stresses over 50 kPa induced by applying an internal pressure of 13.32 kPa in the 17 mm one-compartment simplified tunica albuginea model are shown in Fig. 5(*b*). We can clearly see that significantly different EVM stress distributions were generated in these two models even with the same internal pressure of 13.32 kPa.

The FE analysis results induced by a variety of inputs based on the 12 mm 3D two-compartment diverging model and its related models are summarized in Table 1. As expected, there is a difference in the peak EVM stress between modeling the penis as a one-compartment pressurized vessel and a two-compartment pressurized vessel. An internal pressure of 13.32 kPa induced remarkable differences in the peak EVM stress in the 12 mm two-compartment diverging vessel model and 17 mm one-compartment and 24 mm one-compartment pressurized vessel models. As observed in Table 1, the highest stresses were found in the 24 mm one-compartment pressurized vessel with the same total circumference, with a peak EVM of 100 kPa. All peak stresses for all three models, however, were well below the critical stress (σ_{crit}) of the tunica albuginea, which is 200 kPa.

When a relatively small lateral force of 0.5 N was applied at the tip of the simplified penile models, it was observed that the 17 mm one-compartment and 24 mm one-compartment pressurized

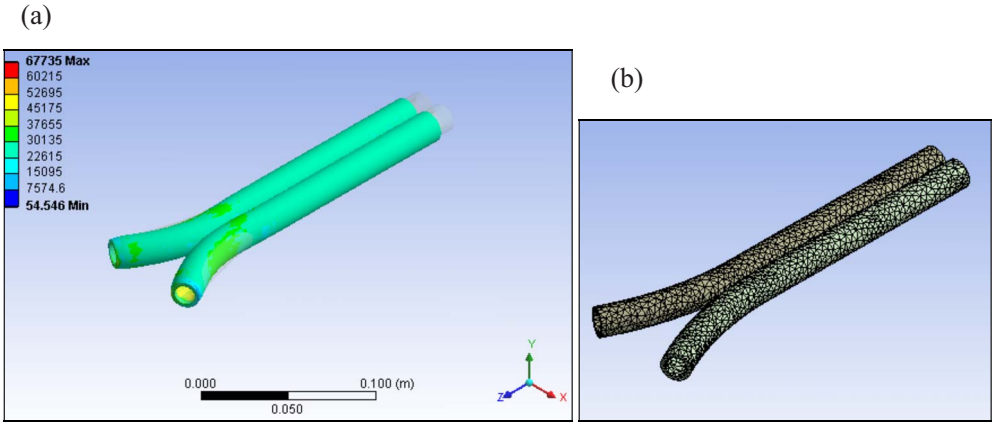

Fig. 4 (*a*) The EVM stress distributions throughout the 12 mm 3D two-compartment diverging model induced by an internal pressure of 13.32 kPa. (*b*) FE mesh of the 12 mm two-compartment diverging model using a tetrahedron solid element for a total of 50,360 elements and 95,651 nodes.

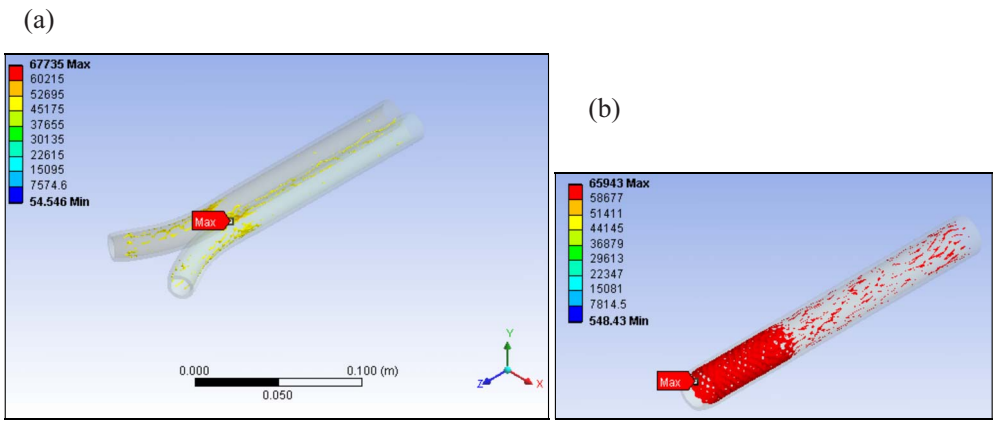

Fig. 5 (a) Distributions of the EVM stresses over 50 kPa induced by applying an internal pressure of 13.32 kPa in (*a*) the 12 mm two-compartment diverging simplified tunica albuginea model and (*b*) the 17 mm one-compartment simplified tunica albuginea model

vessels experienced a higher peak EVM stress than the 12 mm two-compartment diverging vessel, as seen in Table 1. It can also be seen in Table 2 that the percent increase in the peak EVM stress due to the lateral force in the 17 mm and 24 mm one-compartment pressurized vessels is also higher than that of the 12 mm two-compartment diverging vessel. Moreover, the 17 mm one-compartment pressurized vessel model experienced stresses as high as 222 kPa, which exceeds the critical stress of the tunica albuginea. Consequently, Table 1 shows that there was also larger lateral deformation in the direction of the force applied when looking at the one-compartment vessels in comparison to the two-compartment diverging vessel.

The buckling load was also investigated for each model in this study. For vaginal penetration, it is necessary to reach a penile rigidity of 5 N or 500 g of force without bending [12]. As seen in Table 1, the results demonstrated that all three models have a higher buckling load than the minimum, and thus intromission is possible for all three.

It was also observed that the peak EVM stress in the 12 mm two-compartment model was concentrated around the curvature of the tunica albuginea, specifically at the 3 and 9 o'clock locations. However, in the 17 mm one-compartment model, the maximum stresses exceeding 50 kPa were observed throughout the pressurized vessel and covered a more predominant area than in the two-compartment model.

3.2 Physical Penile Models and Validation Results. The lateral deformation test for each of the physical models (10 mm, 12 mm, 14 mm, and their equivalent one-compartment models) was performed once the sleeve was firmly attached to the H_2O column manometer. After applying a 0.5 N lateral force at the tip of the physical model, recording the displacement of the tip, and repeating the test five times for each model, the results were compiled in Table 3 and graphed in Figs. 6(*a*) and 6(*b*). On the same graph, the results from the FE models were graphed in order to compare the two sets of data side-by-side. The standard error was calculated for the five measurements taken for each model, as well as the relative error between the physical model measurements and the FE penile model results in order to validate the results.

3.3 Advanced Anatomically FE Penile Model. The most anatomically correct penile model, which includes the skin, tunica albuginea, and corpus cavernosa, was developed by Gefen et al. in 2002. The stress distribution results based on this penile model in 2D is shown in Fig. 7, which is subjected to an internal pressure Pi. However, a major limitation of this model is that it is a 2D penile model. In the present study, the most anatomically correct 3D penile model has been constructed by extruding the 2D penile model developed by Gefen et al. (Figs. 8(*a*) and 8(*b*)).

FE analysis was conducted based on this 3D penile model after fixing the two proximal ends and applying an internal pressure of 13.32 kPa to the corporal cavernosal bodies, and the FE analysis results are shown in Fig. 8(*b*). The peak EVM stress was found to be about 149 kPa. Using the BUCKLING ANALYSIS feature in ANSYS, the buckling load for this model was found to be 11.82 N (1182 g of force). It can also be seen that the tunica albuginea is indeed the load bearing tissue in the penis since the skin experienced relatively small stresses as a result of the simulated erection. We then removed the septum between the two corporal bodies and remodeled the penis as a one-compartment pressurized vessel to investigate the difference between two- and one-compartment models in the most anatomically correct case. FE analysis results based on the one-compartment penile model show a peak EVM stress as high as 455 kPa in the tunica albuginea (Fig. 9).

4 Discussion and Conclusions

The objective of this study is to investigate the difference between modeling the penis as a one-compartment pressurized ves-

Table 1 Results collected for each model

Model	Peak EVM stress (Pa)	Peak EVM stress axial force (5 N) (Pa)	Peak EVM stress lateral force (0.5 N) (Pa)	Lateral deformation (mm)	Buckling load (N)
12 mm two-compartment diverging	67,735	96,906	99,052	5	13.44
17 mm one-compartment	65,943	87,103	220,600	21	10.71
24 mm one-compartment	85,212	99,995	138,860	9	79.80

Table 2 The percent increase in peak EVM stresses due to a lateral force of 0.5 N

Model	Increase of peak EVM stress (%)
12 mm two-compartment diverging	31.62
17 mm one-compartment	70.11
24 mm one-compartment	38.63

sel and the more anatomically correct two-compartment pressurized vessel. Before attempting to model complex anatomical geometries of the penis, simplified geometric models were designed in which the penile corporal bodies were shaped into pressurized cylinders. In this way, corresponding physical models were successfully constructed and experimental measurements from these physical models were used as validation data to evaluate the performance of the FE modeling approach used to model the penis in this study. As a result in comparing the lateral deformation in the FE model results with the experimental measurements (Figs. 6(*a*) and 6(*b*)), it is evident that the lateral deformation of the penile body decreases as the diameter of the corporal bodies increases in both models. The relative error between the physical penile model and the FE penile model ranged from 10.8% to 43.1% (Table 3), with an average relative error of 23.3% for all nine models. Given that the experimental results were derived from penile models fabricated with material similar to that of the penile tissue, high relative error values were expected and therefore deemed acceptable. Thus, the modeling approach used to model the simplified geometries of the penile models was validated by the corresponding physical models and was ready to be used in modeling more complex and anatomically accurate geometries of the penis.

Distinct differences were observed between the one-compartment pressurized vessel and two-compartment pressurized

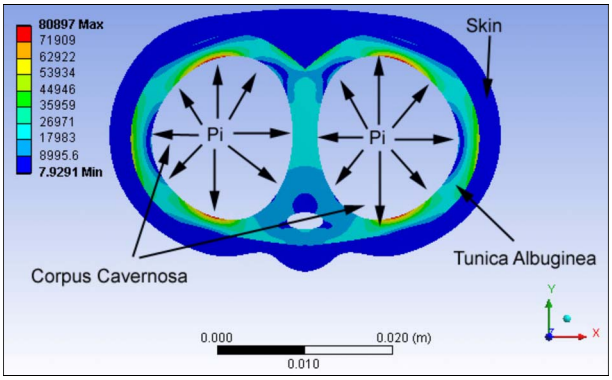

Fig. 7 A more anatomically correct 2D FE model developed by Gefen et al. in 2002 with an internal pressure (Pi) of 13.32 kPa, and the material properties of the skin and tunica albuginea (from Ref. [10], with permission of the International Journal of Impotence Research)

vessels when looking at the von Mises stress distributions and the peak EVM stresses. The buckling loads also varied between these two pressurized models as observed in Table 1, yet based on buckling load analysis both the one- and two-compartment pressurized vessels would be capable of vaginal intromission (which requires a minimum buckling load of 5 N or 500 g of force).

The most significant difference between the two models was evident when external lateral forces were applied. For example, when comparing the two-compartment diverging and the one-compartment same circumference pressurized models, there is a clear difference in the peak EVM stress distribution. In the latter, the tunica albuginea is subject to a more predominant area of peak stresses (Figs. 5(*a*) and 5(*b*)). These results suggest that simplifying the penis geometry to a single pressurized vessel (or an iso-

Table 3 Lateral deformation calculations for physical penile models versus FE penile models

Model	14.1	17	19.8	20	24	28	10 diverging	12 diverging	14 diverging
Mean lateral deformation (mm)	36.2	25.8	17.0	15.8	12.4	7.20	7.80	6.60	4.20
FEA lateral deformation (mm)	36.7	21.0	14.5	15.2	9.00	6.12	6.3	4.61	3.34
Standard error (±)	0.58	0.96	0.54	0.73	0.40	0.37	0.37	0.4	0.37
Relative error (%)	10.79	22.97	17.33	11.64	37.75	17.58	22.76	43.10	25.68

(a)

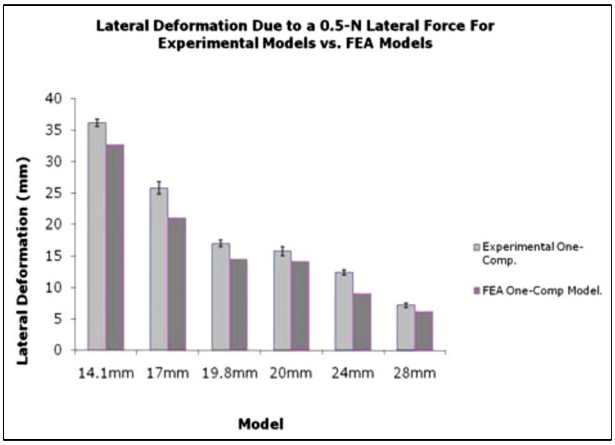

(b)

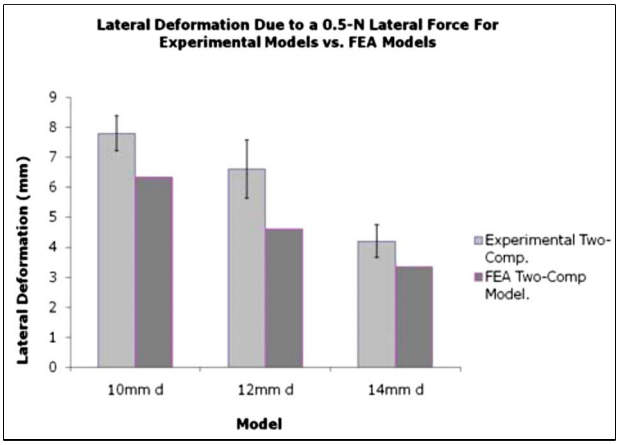

Fig. 6 (*a*) Comparison of lateral deformation induced by applying a 0.5 N lateral force in the one-compartment pressurized vessel model and the corresponding physical model. (*b*) Comparison of lateral deformation induced by applying a 0.5 N lateral force in the two-compartment pressurized vessel model and the corresponding physical model.

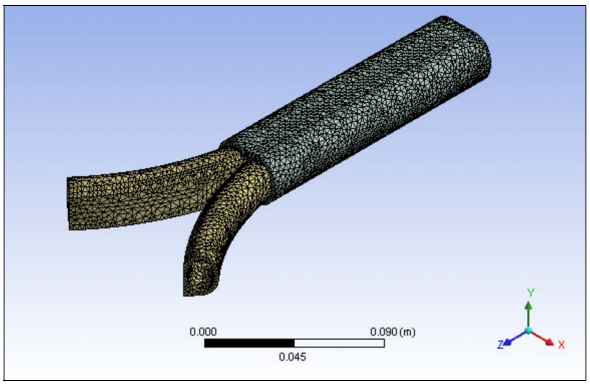

(a)

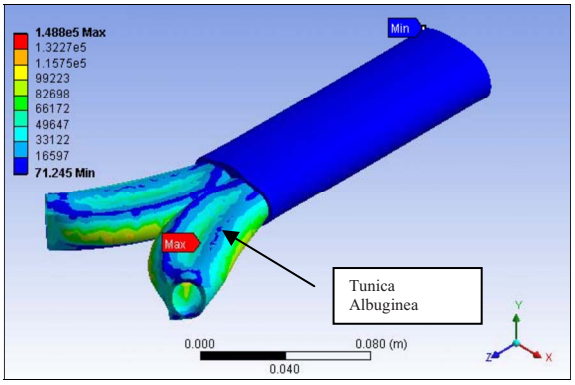

(b)

Fig. 8 (*a*) FE mesh of the more anatomically correct 3D penile model and (*b*) the EVM stress distributions of the more anatomically correct 3D penile model, as a result of fixing the two proximal ends and applying an internal pressure of 13.32 kPa to the corporal cavernosal bodies

tropic shaft) will yield inaccurate results as to how the penis will realistically experience stress distributions as well as its buckling load and its lateral deformation due to external forces. It was also observed that there was a difference in the von Mises stress distribution as well as in the peak EVM stress when considering the geometry of the penis sections inside and outside the body due to the curvature in the corporal cavernosal bodies as they diverge and attach at the pubic arch. Hence, future biomechanical models of the penis should not only consider modeling the penis as a two-compartment pressurized vessel but must also consider the proximal diverging characteristic of the corporal bodies.

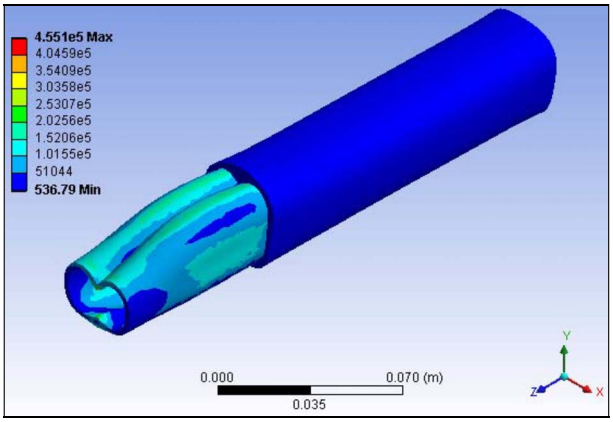

Fig. 9 The EVM stress distributions of the modified one-compartment 3D model of the more anatomically correct penile model as a result of removing the perforated septum that separates the corporal bodies, fixing the model at one end, and applying an internal pressure of 13.32 kPa

Furthermore, it was interesting to observe that the peak EVM stress was mostly concentrated around the inner curvature of the corporal bodies (3 and 9 o'clock positions of the right and left corpus cavernosa, respectively) in the two-compartment diverging pressurized models (Fig. 5(*a*)). A study has shown that most of the reported penile fractures indeed initiate at this relatively thin region (3 or 9 o'clock) [8]. It would be interesting and clinically important to pursue a further study in which rupturing of the tunica albuginea occurs and to correlate these results with those of the peak EVM stress achieved based on the penile model. In this study, the models suggested that there is indeed a correlation between the location of the rupture and the curvature of the tunica albuginea as it enters and diverges inside the body.

Most cases, in which blunt trauma is the cause of impotence, occur when the penis slips out of the vagina and is subsequently thrust against the partner's pubic bone during intercourse or during masturbation due to abnormal bending [1]. In order to simulate these cases, a relatively small lateral force was applied to the penile models. Through a corresponding FE analysis, we found that the peak EVM stress in the one-compartment pressurized vessel increased considerably, exceeding the σ_{crit} of the tunica albuginea. This indicates that a one-compartment pressurized vessel is highly unstable under lateral forces and suggests that rupturing of the tunica albuginea might very well occur in this situation. On the other hand, the peak EVM stress in the two-compartment diverging pressurized vessels remained much lower than the σ_{crit}, as observed in Tables 1 and 2. Hence, this study clearly indicates that the two-compartment pressurized vessel has greater structural integrity than the one-compartment pressurized vessel when subjected to external forces. Therefore, it is fair to speculate that for this reason the anatomical configuration in which the penis has two pressurized corporal bodies instead of one is favored due to decreased susceptibility to injury.

We also found that when we removed the perforated septum that separates the two corporal bodies in the more anatomically correct penile model (Fig. 9), the simulated peak EVM stress increased to 455 kPa, well beyond the σ_{crit} of the tunica albuginea, which is 200 kPa. These extremely high stresses were partly due to the large increase in the hoop stress as a result of removing the septum and increasing the inner radius of the compartment. This finding reinforced the observation that there is indeed a difference between modeling the penis as a one-compartment pressurized vessel and the more anatomically correct two-compartment pressurized vessel. It also clearly shows that the anatomy of the penis with two corporal cavernosal bodies separated by a perforated septum is key to the structural integrity of the tunica albuginea since having one corporal body would result in the rupturing of the tunica albuginea once full erection is achieved.

This study modeled the penis in 3D with two corpora cavernosal bodies fixed at the pelvic arch. The advanced anatomical FE penile model developed in this study represents the most comprehensive penile model in the erectile function research field. However, the biomechanical model of the penis can still be improved in order to enhance the understanding of normal erectile functions, erectile dysfunction conditions, and associated alternative treatments. For example, Zhang et al. developed a computer modeling approach for modeling human organ systems using the subject's specific magnetoresistant (MR) images [15]. Similarly, a more realistic geometric penile model could be developed from the MR images of the penis to include more anatomical details [16]. Additionally, we are performing biomechanical testing procedures on soft tissue specimens harvested from fresh cadavers to develop a soft tissue property database. Upon completion of this soft tissue property database, the penile model could be further refined by using viscoelastic material properties for the penile tissues in-

volved in the penile models [17–19]. Results based on refined penile models would more accurately represent the biomechanical behavior of the penis [20–23].

In conclusion, a significant difference was demonstrated between modeling the penis as a two- versus a one-compartment pressurized vessel. Based on this finding, an advanced anatomical penile model has been developed to generate more accurate simulation results of the biomechanical behavior of the penis. Additionally, a distinct advantage was observed by having two corporal based cavernosal bodies separated by a perforated septum that diverge as they enter the body and attach at two separate points, as opposed to one corporal body attached at one end. This is due to the better structural integrity of the tunica albuginea when subjected to external forces, specifically lateral forces.

Acknowledgment

This work was supported by the University of Minnesota Supercomputing Institute, the Institute for Engineering in Medicine, the Department of Mechanical Engineering, and the Department of Urologic Surgery at the University of Minnesota. The authors would like to thank Dr. Yingchun Zhang for his help in reviewing and editing the manuscript.

References

[1] Gefen, A., Chen, J., and Elad, D., 2001, "Computational Tools in Rehabilitation of Erectile Dysfunction," Med. Eng. Phys., **23**(2), pp. 69–82.
[2] Kandeel, F., Koussa, V., and Swerdloff, R., 2001, "Male Sexual Function and Its Disorders: Physiology, Pathophysiology, Clinical Investigation and Treatment," Endocr. Rev., **22**(3), pp. 342–388.
[3] Lakin, M., 2005, "Erectile Dysfunction," The Cleveland Clinic Medicine Index, The Cleveland Clinic Foundation, http://www.clevelandclinicmeded.com/medicalpubs/diseasemanagement/endocrinology/erectile/erectile.htm
[4] Udelson, D., 2007, "Biomechanics of Male Erectile Function," J. R. Soc., Interface, **4**, pp. 1031–1047.
[5] 2005, "Erectile Dysfunction," National Kidney and Urologic Diseases Information Clearinghouse, "Lifestyle Changes Improve Erectile Function," American Diabetes Association, http://kidney.niddk.nih.gov/kudiseases/pubs/impotence /#cause
[6] Elayaperumal, S., Timm, G., and Hegrenes, J., 2007, "Biomechanical Analysis of Erectile Function: Penile Buckling Behavior Under Axial Loading and Radial Compression," Br. J. Urol., **102**, pp. 76–84.
[7] Hellstorm, W., and Bivalacua, T., 2000, "Peyronie's Disease: Etiology, Medical and Surgical Therapy," J. Androl, **21**(3), pp. 347–354.
[8] Brock, G., Hsu, G. L., Nunes, L., von Heyden, B., and Lue, T., 1997, "The Anatomy of the Tunica Albuginea in the Normal Penis and Peyronie's Disease," J. Urol., **157**, pp. 276–281.
[9] Bitsch, M., Kromann-Andersen, B., Schou, J., and Sjøntoft, E., 1990, "The Elasticity and the Tensile Strength of Tunica Albuginea of the Corpora Cavernosa," J. Urol., **143**, pp. 642–645.
[10] Gefen, A., Elad, D., and Chen, J., 2002, "Biomechanical Aspects of Peyronie's Disease in Development Stages and Following Reconstructive Surgeries," Int. J. Impot Res., **14**, pp. 389–396.
[11] Linder-Ganz, E., Gefen, A., Elad, D., and Chen, J., 2007, "A Three Dimensional Model of the Penis for Analysis of Tissue Stresses During Normal and Abnormal Erection," Ann. N.Y. Acad. Sci., **1101**, pp. 464–476.
[12] 2008, "Linear Elastic Material Behavior," Constitutive Models-Relations Between Stress and Strain, Applied Mechanics of Solids, http://solidmechanics.org/text/Chapter3_2/Chapter3_2.htm#Sect3_2_1
[13] "Hydrostatic and Deviatoric Stress: von Mises Effective Stress," 2008, Governing Equations, Applied Mechanics of Solids, http://solidmechanics.org/text/Chapter2_2/Chapter2_2.htm#Sect2_2_7
[14] Gefen, A., Elad, D., and Chen, J., 2000, "A Biomechanical Model of Peyronie's Disease," J. Biomech., **33**(12), pp. 1739–1744.
[15] Zhang, Y., Sweet, R. M., Metzger, G. J., Burke, D. M., Erdman, A. G., and Timm, G. W., 2009, "Advanced Finite Element Mesh Model of Female SUI Research During Physical and Daily Activities," Stud. Health Technol. Inform., **142**, pp. 447–452.
[16] Gefen, A., Chen, J., and Elad, D., 1999, "Stresses in the Normal and Diabetic Human Penis Following Implantation of an Inflatable Prosthesis," Med. Biol. Eng. Comput., **37**, pp. 625–631.
[17] American Medical Systems, 2005 "Erectile Dysfunction," AMS Solutions for Life, http://www.visitams.com/conditions_treatments_detail _objectname_mens_ed.html
[18] 2004, "About Penis Enlargement Methods," Penile Anatomy, Penis Hints, http://www.penishints.com/about-penis-enlargement.htm
[19] 2005, "Vig-RX's How Does It Work," Anatomy of the Penis, Vid-RX. 2, http://www.vig-rxreview.com/about.html
[20] Shirai, M., Ishii, N., Mitsukawa, S., Matsuda, S., and Nakamura, M., 1978, "Homodynamic Mechanism of Erection in the Human Penis," Systems Biology in Reproductive Medicine, **1**(4), pp. 345–349.
[21] El-Sakka, A., 2003, "Association Between International Index of Erectile Function and Axial Penile Rigidity in Patients With Erectile Dysfunction," Int. J. Impot Res., **15**, pp. 426–429.
[22] Hibbeler, R., 2007, *Mechanics of Materials*, Pearson, Upper Saddle River, New Jersey.
[23] Budynas, R., and Nisbett, K., 2006, *Shigley's Mechanical Engineering Design*, McGraw-Hill, New York.